Baseline measurements for testing of improved triple-sensor hot-wire anemometer probe in a momentum conserving turbulent round jet

F. Gökhan Ergin
Dantec Dynamics A/S, Skovlunde, DK
gokhan.ergin@dantecdynamics.com

Clara Marika Velte
Department of Mechanical Engineering
Technical University of Denmark
Kgs. Lyngby, DK
cmve@dtu.dk

ABSTRACT

Three-component velocity measurements have been performed in a momentum conserving turbulent round jet using a constant-temperature anemometer (CTA) system and a new triple-sensor probe featuring straight prongs. The objective is to test the reliability of the new probe in a classical canonical flow that lends itself well to testing physical quantities such as momentum flux conservation as well as comparing directly to baseline data. The probe is positioned in excess of 2500 positions in each measurement plane using a computer controlled traversing mechanism. A conventional two-step calibration is performed where the directional calibration is conducted following a velocity calibration. The calculated pitch and yaw factors are compared to expected values for similar probes reported in the literature. An error analysis is performed using the pitch / yaw - roll mechanism in order to identify the acceptance angle for the probe for the data reduction scheme. The measurements capture the main well-known characteristics of the round jet such as the jet centerline, jet half width, and virtual origin. Power spectra were measured at 30 jet exit diameters downstream of the jet exit on the jet centerline, quarter-width, half-width, three-quarters width and at full jet width, demonstrating the variations in the dynamic statistical moments.

EXPERIMENTAL SETUP

The experimental setup is shown in Fig. 1. The jet is the light blue cubic box of dimensions 58 x 58.5 x 59 cm^3 fitted with an axisymmetric white plexiglass nozzle, tooled into a fifth-order polynomial contraction from an interior diameter of 6 cm to an exit diameter of D = 1 cm. The interior of the box was stacked with foam baffles in order to damp out disturbances from the fan that supplied the generator with pressurized air. The air intake was located inside the jet enclosure. For further details on the generator box, see Jung et al. (2004) and Gamard et al. (2004). The exit velocity is monitored via a pressure tap in the nozzle positioned upstream of the contraction and connected to a digital manometer by a silicon tube. The enclosure was a large tent of dimension 2.5 x 3 x 10 m^3. The jet was the same as that used by Ewing et al. (2007) and the enclosure was similar as well. Under these conditions, the jet flow generated in the facility should be expected to correspond to a free jet up until x/D = 70 from the jet exit, which is sufficient for the purpose of the measurements performed herein. However, the probe is positioned using a computer controlled traversing mechanism (Fig. 1, on the left), which occupies substantial amount of space in the enclosure. This may lead to the fact that the momentum conservation may fail in particular in the outer edges of the measured profiles of the round jet (Hussein et al. 1994).

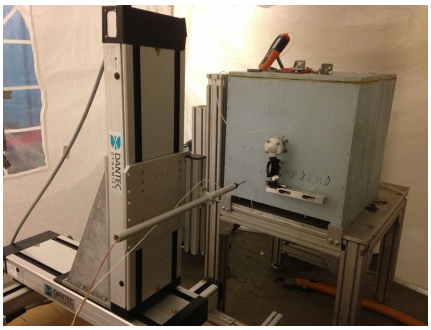

Figure 1 Jet facility, hot-wire probe and 3-axis traversing mechanism. For practical reasons, flow blockage due to the traversing system is difficult to avoid. This has been countered by placing the probe on a lengthy, but stable, extension arm to increase the distance between traversing system and probe.

The measurement system is a constant-temperature anemometer (CTA) system manufactured by Dantec Dynamics (DD, Skovlunde Denmark). The system consists of a StreamLine Pro Frame and Controller with three CTA velocity channels, StreamLine Pro Automatic Calibrator with Nozzle I, a Pitch/Yaw – Roll (PYR) manipulator to perform directional calibrations and StreamWare Pro software. The system controller is a Dell Precision T1600 PC with an Intel Xeon E31245 3.3Ghz CPU and 8GB Ram, running on a 64-bit Windows 7 Ultimate operating system. The measured voltages were transferred to the computer via a National Instruments connector box and an 8-channel simultaneous sampling differential PCI A/D converter. The new 55P95 triple-wire probe is positioned at multiple grid points using a

computer-controlled 3-axis traversing system. The probe is compatible with the 55H27 triple sensor probe support, and was mounted on the traversing mechanism using this support and a mechanical adapter.

The probe (Fig. 2) was placed in the (vertical) calibration jet during the velocity calibration. Nozzle I was used to cover a velocity range of 1-60 m/s. For accurate three-component measurements, an accurate directional calibration was also performed using a pitch/yaw-roll manipulator. During the directional calibration, the probe is yawed and rolled around two axes, while it is exposed to a constant calibration velocity, which is half of the maximum velocity during velocity calibration. Measuring the probe response with the actual velocity on each sensor, the pitch and yaw factors are calculated. Individual velocity and directional calibrations improve the accuracy of the measurement compared to experiments using standard pitch & yaw factors.

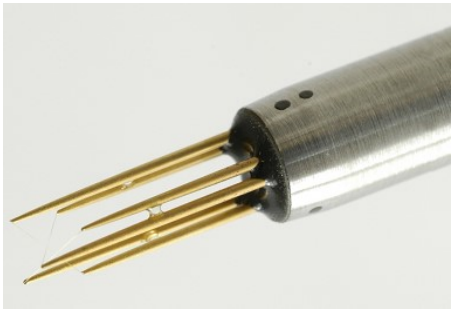

Figure 2 Novel triple-sensor probe with straight prongs.

CALIBRATION OF THE NEW PROBE 55P95

The calibration of the new 55P95 probe is a two-step procedure. First, a velocity calibration is performed from 1 m/s to 50 m/s using Nozzle I at 10 points distributed equally in the velocity range. Then, a directional calibration is performed with constant jet speed of 25 m/s with a 30 deg yaw angle and in steps of 15 deg roll angle. The measured pitch and yaw factors are summarised in Table 1, and are consistent with the expected values reported previously for 55P91.

Table 1 Measured and expected pitch/yaw coefficients for new 55P95 sensors

Measured	k^2	h^2
Wire 1	0,0112	1,0092
Wire 2	0,0395	1,0180
Wire 3	0,0226	1,0327
Expected	0,025	1,04

Following calibration, the measurement accuracy of the new probe is verified using the calibration jet and the pitch/yaw manipulator. When the probe is placed vertically in the laminar calibration jet, the probe is expected to detect exclusively the streamwise velocity component, as the other two velocity components should be negligible in comparison. Similarly, when the probe is yawed in x-y plane and in x-z plane, the probe is expected to detect negligible velocities in w- and v-components, respectively. The absolute measurement error variation (%) with the acceptance angle at a constant jet speed of 25 m/s is given in Figure 3. The absolute measurement error is <5% for yaw angles < 20 deg and < 10% for yaw angles < 30 deg. This means that this probe's full acceptance cone angle is 60 deg with the data reduction scheme described herein.

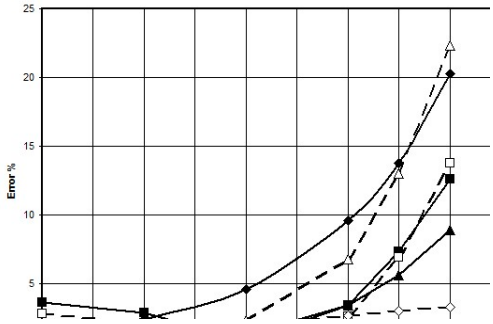

Figure 3 Error variation with incidence angle.

RESULTS

Measurements have been performed throughout cross-planes with 51 x 51 measurement points each at 9 downstream positions. The measurement plane side length was expanded according to the downstream jet growth-rate. The equidistantly spaced planes covered a downstream span of 10D – 50D, where D is the jet exit diameter. Up to 30D, the jet is classically considered only partially developed in the sense that the mean velocities are self-similar while the second order statistical moments only become fully developed from about 30D and beyond. The jet can, to within reasonable approximation, be considered free and momentum conserving within the downstream range covered. At 50D the ratio between the local jet momentum to the momentum at the nozzle $M/M_0 \approx 0.997$ (based on eqn. B10 in Hussein et al. 1994).

Fig. 4 displays the downstream evolution of the measured streamwise velocity profiles. Further, lines roughly indicating the jet centerline and the linearly growing jet half-width (where the mean streamwise velocity has dropped to half the centerline value) are included for guidance of the reader.

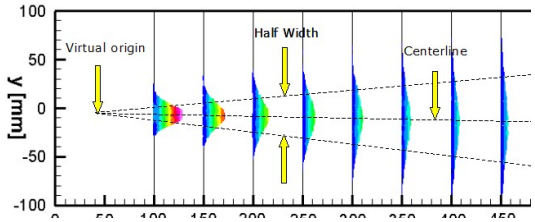

Figure 4 Jet profile development in the downstream direction x. The nozzle is located at x,y=0.

It is apparent from Fig. 4 that the jet centerline and the downstream traversing direction are slightly misaligned. The (developed) jet half-width follows $\delta_{1/2}/(x-x_o)\sim0.09$. The virtual jet origin is determined from extrapolation to $x_0/D=4$.

Correcting for the traversing system misalignment to the jet development, the measurements are transferred into

a polar coordinate system and analysed, see Figure 5(a). Since the mean velocity becomes self-similar before x=30D, all radial velocity profiles are expected to collapse if scaled correctly, which is also observed in the measurements, see Figure 5(b). Since each jet may develop differently because of the turbulence dependency upon initial conditions (George 2012), the provided comparison to fittings from alternative data should not be considered too seriously. Comparison should rather be made to reliable data acquired for the very same jet flow (such as PIV or LDA measurement data).

The centreline velocity development is plotted in Figure 5(c). Again, the virtual origin of the jet is found to be $x_0/D = 4$ while the decay rate $B_u = 7.1$ for this particular jet flow (Hussein et al. 1994) where:

$$U_c = \frac{B_u \cdot M_0^{1/2}}{(x - x_0)}$$

$M_0 = \pi(d/2)^2 \rho U_0 = 0.0866\ kg\ m/s^2$ is the momentum flux at the jet exit and $U_0 = 30\ m/s$ is the jet exit velocity. The momentum flux for a free jet is conserved with downstream distance so long as the enclosure is not too small or other disturbances too large to create significant back-flow and other secondary effects (Hussein et al. 1994):

$$M(x) = M_0 = 2\pi \int_0^\infty \left[U^2 + \overline{u^2} - \frac{1}{2}\left(\overline{v^2} + \overline{w^2}\right) \right] r\, dr$$

Since the jet half-width $\delta_{1/2}=0.09(x-x_0)$ the product $U_c\ \delta_{1/2} = B_u\ M_0^{1/2}\ 0.09 = B_u\ M^{1/2}(x)\ 0.09 = constant$. This has been tested in Figure 5(d), where good agreement has been achieved except for x/D = 45 and 55 where it is believed that the spatial extent of the measuring plane may have been too narrow to capture all the energy in the flow. Reducing the momentum flux expression to first order (removing the second order moments) displays negligible impact on the result.

The measured velocity power spectra for u, v, and w at x=30D on the jet centerline, at quarter jet width, at half jet width, ¾ jet width, and at full jet width are shown in Fig. 6. The results show a distinctly non-isotropic behaviour at lower frequencies (<100Hz) with the axial turbulent kinetic energy being an order of magnitude higher than the secondary components. The higher frequencies collapse with increased radial distance from the jet centreline as is expected for temporal spectra in high intensity jet flows (Lumley 1965).

CONCLUSIONS

The new probe design produces accurate directional calibrations by eliminating the prong effects observed for previous designs. As a direct result of this, the reconstructed 3D velocity vector is more accurate within the acceptance cone of the probe – approximately 60 deg for the current prong configuration and data reduction scheme.

The streamwise velocity profiles at each downstream position were plotted in regular and similarity scaling variables, displaying clear similarity collapse of the mean velocity even as far upstream as x/D=10. Due to the turbulence dependency upon initial conditions, the profile could not be quantitatively validated against other jet measurements, although it was seen that the measurements in general displayed the expected trends. The jet expansion and centreline velocity developments were determined from the data and a multiple check of the momentum flux conservation was performed. The results indicated a general agreement, even though some spurious points existed that were hypothesized to stem from the differences in measurement plane extent. The full momentum flux can naturally not be captured unless the full region of non-zero momentum flux is covered in the measurements.

The measured power spectra capture the expected characteristics even at large distances from the jet centreline where the turbulence intensity is exceptionally high. These spectra will in the future be compared to high-precision laser Doppler anemometer (LDA) power spectra for validation of the novel hot-wire probe design. The LDA does not suffer from directional ambiguity and can provide a valuable and unbiased baseline as long as correct signal processing is implemented for extracting static and dynamic statistical moments (Velte *et al.* 2014).

Further, static moments such as mean velocity, rms values etc. measured with the novel hot-wire probe will be compared to corresponding LDA measurements in the same jet facility. In particular, the comparison will focus on the challenging case of high turbulence intensity in the outer parts of the jet where hot-wire probes have classically had significant difficulties in producing reliable results. Future work also includes the comparison of different directional calibration schemes for reduced error over a larger acceptance angle.

ACKNOWLEDGMENTS

The authors are grateful to Mr. Carsten Pedersen for software implementation.

REFERENCES

Ewing D, Frohnapfel B, George WK, Pedersen JM, Westerweel J (2007) Two-point similarity in the round jet. Journal of Fluid Mechanics, 557:309330.

Gamard S, Jung D, George WK (2004) Downstream evolution of the most energetic modes in a turbulent axisymmetric jet at high Reynolds number. Part 2: The far-field region. Journal of Fluid Mechanics, 514, 205-230.

H.J. Hussein, S.P. Capp, and W.K. George. Velocity measurements in a high-Reynolds-number, momentum-conserving, axisymmetric, turbulent jet. J. Fluid Mech. 258: 31–75, 1994.

Jung D, Gamard S, George WK (2004) Downstream evolution of the most energetic modes in a turbulent axisymmetric jet at high Reynolds number. Part 1: The near-field region. Journal of Fluid Mechanics, 514, 173-204.

George, W. K. (2012). Asymptotic effect of initial and upstream conditions on turbulence. Journal of Fluids Engineering, 134. 061203-1

Lumley, J. L. (1965). Interpretation of time spectra measured in high intensity shear flows. Physics of Fluids, 8, 1056. Doi: 10.1063/1.1761355

Velte, C. M. et al. (2014). Estimation of burst-mode LDA power spectra. Experiments in Fluids, 55:1674. DOI 10.1007/s00348-014-1674-z

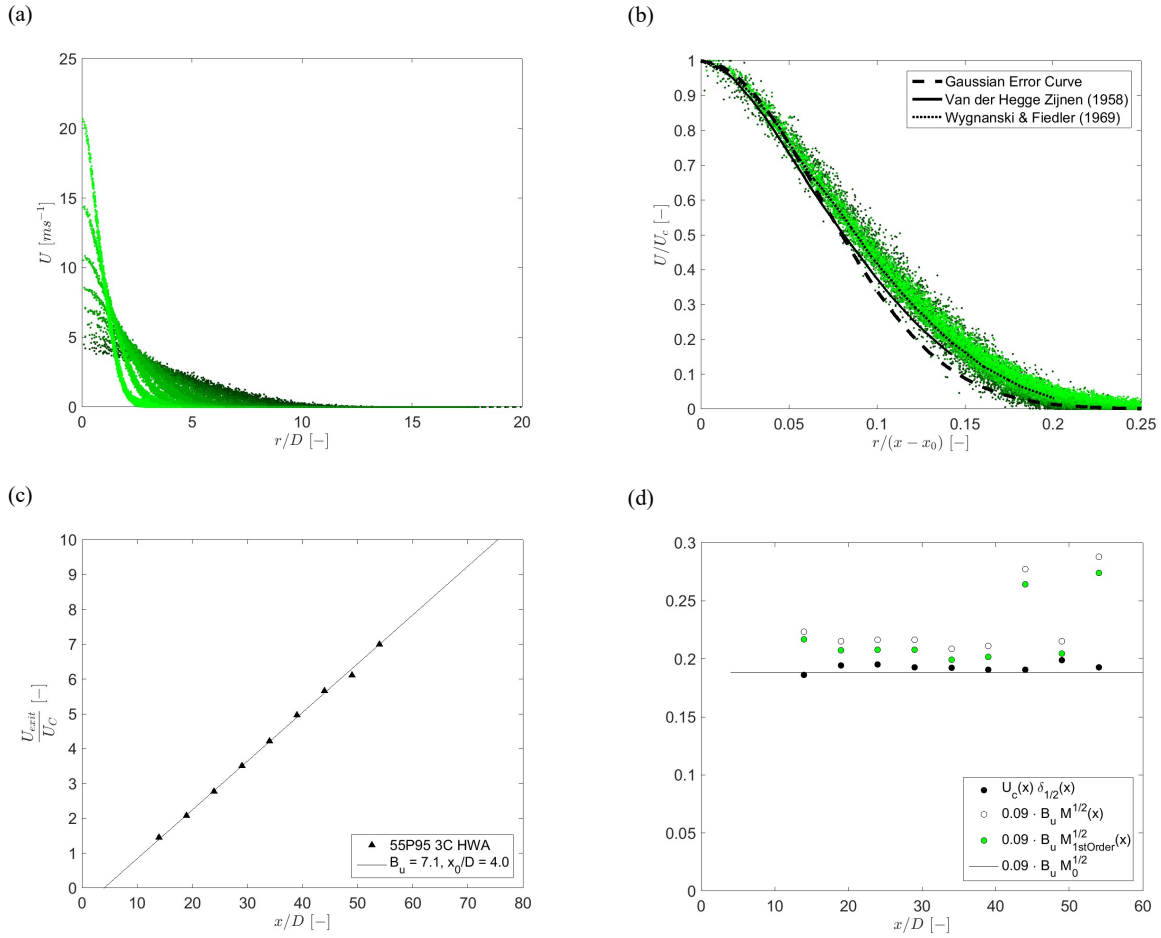

Figure 5 Streamwise velocity (u) profiles at all measured downstream positions x/D = 10, 15, 20, 25, 30, 35, 40, 45 & 50. Darker green corresponds to larger downstream distance. (a) Unscaled velocity profiles. (b) Similarity scaled velocity profiles. (c) Centerline velocity downstream development. (d) Check of consistency for momentum flux conservation.

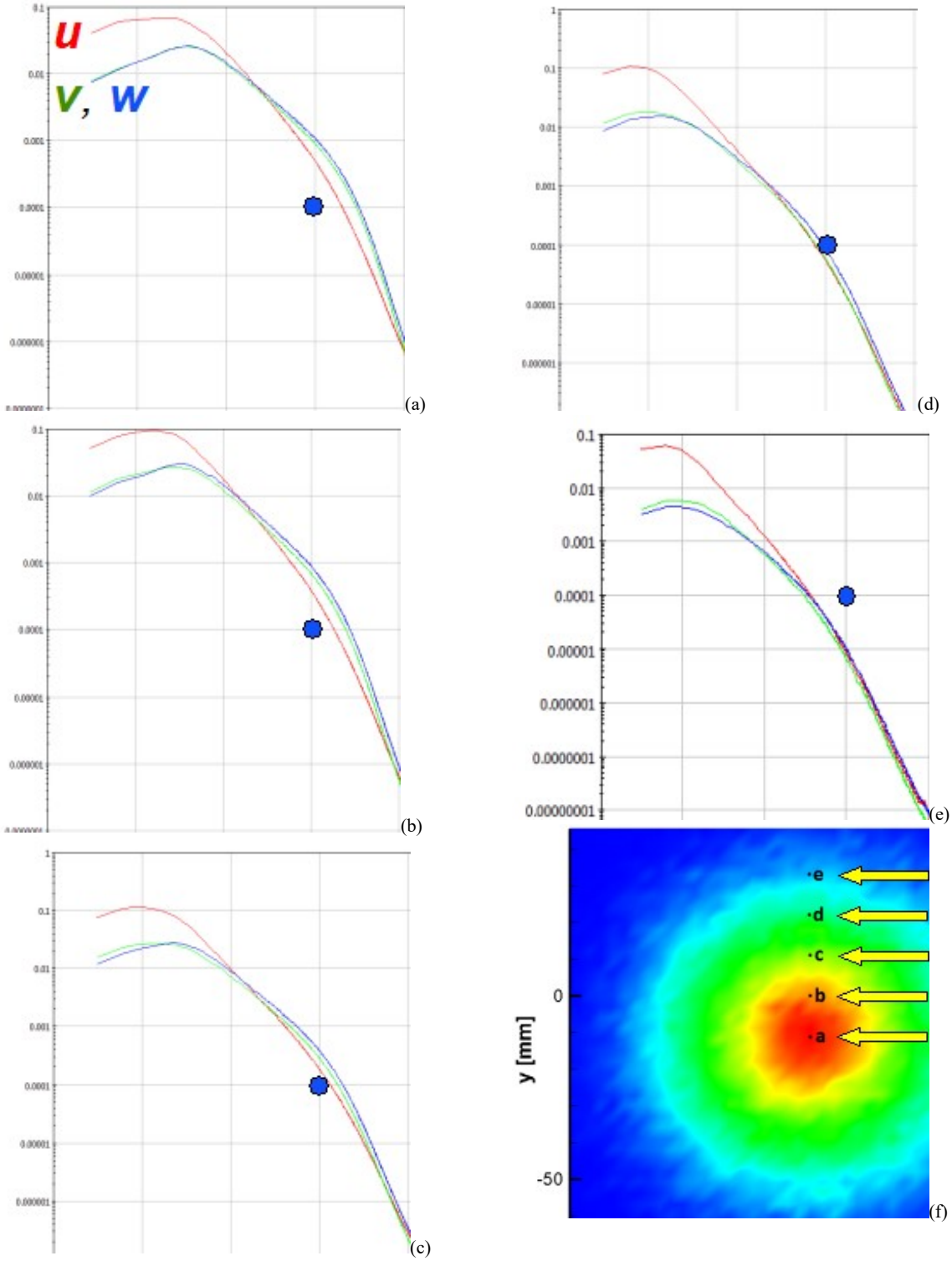

Figure 6 Power spectra for u, v, and w at 30D on (a) the jet centerline, (b) quarter jet width, (c) half jet width, (d) ¾ jet width, (e) jet width, (f) positions of PSD computations at x = 30D.